

Analysis of Regional Travel Time Data from the November 1999 Dead Sea Explosions Observed in Saudi Arabia

*A. Rodgers, A. M. S. Al-Amri, A. Ar-Rajehi, T. Al-Khalifah,
M. S. Al-Amri, M. S. Al-Haddad, N. Al-Arifi*

April 19, 2000

U.S. Department of Energy

Lawrence
Livermore
National
Laboratory

DISCLAIMER

This document was prepared as an account of work sponsored by an agency of the United States Government. Neither the United States Government nor the University of California nor any of their employees, makes any warranty, express or implied, or assumes any legal liability or responsibility for the accuracy, completeness, or usefulness of any information, apparatus, product, or process disclosed, or represents that its use would not infringe privately owned rights. Reference herein to any specific commercial product, process, or service by trade name, trademark, manufacturer, or otherwise, does not necessarily constitute or imply its endorsement, recommendation, or favoring by the United States Government or the University of California. The views and opinions of authors expressed herein do not necessarily state or reflect those of the United States Government or the University of California, and shall not be used for advertising or product endorsement purposes.

This work was performed under the auspices of the U. S. Department of Energy by the University of California, Lawrence Livermore National Laboratory under Contract No. W-7405-Eng-48.

This report has been reproduced
directly from the best available copy.

Available to DOE and DOE contractors from the
Office of Scientific and Technical Information
P.O. Box 62, Oak Ridge, TN 37831
Prices available from (423) 576-8401
<http://apollo.osti.gov/bridge/>

Available to the public from the
National Technical Information Service
U.S. Department of Commerce
5285 Port Royal Rd.,
Springfield, VA 22161
<http://www.ntis.gov/>

OR

Lawrence Livermore National Laboratory
Technical Information Department's Digital Library
<http://www.llnl.gov/tid/Library.html>

Analysis of Regional Travel Time Data from the November 1999 Dead Sea Explosions Observed in Saudi Arabia

Arthur Rodgers¹, Abdullah M.S. Al-Amri², Abdullah Ar-Rajehi³, Tariq Al-Khalifah³, Mohammed S. Al-Amri³, Mohammad S. Al-Haddad⁴ and Nassir Al-Arifi²

¹ *Lawrence Livermore National Laboratory, Earth and Environmental Sciences Directorate, Livermore, CA 94551 USA, rogers7@llnl.gov*

² *Department of Geology and Seismic Studies Center, King Saud University, Riyadh, 11451, Saudi Arabia*

³ *Astronomy and Geophysics Research Institute, King Abdulaziz City for Science and Technology, Riyadh, Saudi Arabia*

⁴ *Department of Civil Engineering, King Saud University, Riyadh, 11421, Saudi Arabia*

Abstract

Two large chemical explosions were detonated in the Dead Sea in order to calibrate seismic travel times and improve location accuracy for the International Monitoring System (IMS) to monitor a Comprehensive Nuclear Test-Ban Treaty (CTBT). These explosions provided calibration data for regional seismic networks in the Middle East. In this paper we report analysis of seismic data from these shots as recorded by two seismic networks run by King Saud University (KSU) and King Abdulaziz City for Science and Technology (KACST) in Saudi Arabia. The shots were well observed in the distance range 180-480 km mostly to the south of the Dead Sea in the Gulf of Aqaba region of northwestern Saudi Arabia. An average one-dimensional velocity model for the paths was inferred from the travel times of the regional phases Pn, Pg and Sg. Short-period Sn phases were not observed. The velocity model features a thin

crust (crustal thickness 26-30 km) and low velocities (average P-wave velocity 5.8-6.0 km/s), consistent with the extensional tectonics of the region and previous studies.

Introduction

In November of 1999, the Geophysical Institute of Israel conducted two large chemical explosions in the Dead Sea. These explosions were conducted to provide calibration data for seismic travel times to stations of the International Monitoring System (IMS) to improve detection and location efforts for Comprehensive Nuclear Test-Ban Treaty (CTBT) monitoring. Details of the shot locations and origin times are compiled in Table 1. A smaller shot (500kg) was conducted on November 8, 1999, but we did not analyze the data because the signal-to-noise was poor on the Saudi networks. The Middle East has dense coverage of seismic stations due to the relatively high population density and earthquake hazard along the Gulf of Aqaba-Dead Sea Rift. Stations operated by two regional networks in Saudi Arabia were operating during the shots. A map of the shot and station locations is shown in Figure 1.

King Saud University (KSU) operates a network of mostly short-period vertical component seismic stations. King Abdulaziz City for Science and Technology (KACST) operates a network of three-component broadband and short-period stations (Al-Amri and Al-Amri, 1999). Both networks have stations throughout the Kingdom of Saudi Arabia, but the station density is greatest near the Gulf of Aqaba. These networks recorded the shots with good signal-to-noise above about 0.5 Hz. Figure 2 shows the vertical component waveforms for the largest shot. The main regional seismic phases Pn, Pg and Sg are clearly visible in most of these traces. Our travel time picks are shown in the figure.

The KACST network collects and processes data in real time. The two large Dead Sea shots were detected and located automatically by the real time system. The automatic locations are shown in Figure 1 and the mislocations from ground truth are given in Table 2. Errors in the automatic locations are 29.1 and 50.7 km for the

November 10 and 11 shots, respectively. While these errors are large it is not surprising because the location was estimated from automatic detections and residuals were computed relative to the *iasp91* velocity model (Kennett and Engdahl, 1991).

In the following, we used the arrival times of the regional phases Pn, Pg and Sg to develop a more appropriate velocity model for the region. Our model is consistent with other seismological estimates of crustal structure in the Dead Sea Rift region. This model can then be used to locate new events in the region.

Velocity Model Development

The travel times of Pn, Pg and Sg were used to develop a velocity model of the crust and uppermost mantle for the Dead Sea Rift region. The crustal S-wave, Sg, is observed on all seismograms, despite the source being an explosion in water. Strong Sg energy may be generated by Rg-to-Sg conversions near the source (Myers et al., 1999). Sn was not clearly observed for these data, including the horizontal components of the KACST network stations. Sn is not expected to propagate efficiently along the paths studied. Previous studies report inefficient Sn propagation in the Dead Sea Rift (Kadinsky-Cade et al., 1986; Rodgers et al., 1997). Inefficient propagation of short-period mantle S-waves probably results from attenuation and is related to low seismic velocities directly below the Moho.

Firstly we regressed the travel times of each phase versus distance. Data from both shots were included in this analysis. The data and regression models and errors are shown in Figure 3. The fact that both explosions have very similar travel times to each station indicates that there are not timing errors at the stations between the two shots. The slopes of the Pg and Sg travel times versus distance should reflect the average P- and S-wave velocities of the crust, while the Pn travel time slope should indicate the average sub-Moho P-wave velocity. However, caution must be exercised because two-dimensional structure along the path could bias the results. In fact analysis of seismic refraction data sampling the Sinai Peninsula margin of the Gulf of Aqaba indicates that

crust thins from about 30 km north of the Gulf to 20 km at the southern-most tip of the Peninsula (Ginzburg et al., 1979). Our goal here is to derive a path-averaged 1D model for the paths considered so that future events can be more accurately located.

The slopes of Pg and Sg imply low average crustal velocities (6.28 km/s and 3.43 km/s or P- and S-waves, respectively), consistent with felsic upper crustal compositions of typical continental sections (Christensen and Mooney, 1995; Rudnick and Fountain, 1995). The average Pn velocity of 7.75 km/s is lower than the global average (8.09 km/s; Christensen and Mooney, 1995) but consistent with the seismic refraction study of Ginzburg et al., (1979) and the Pn tomography study of Hearn and Ni (1994). The absence of short-period Sn propagation in the region and low Pn velocities may be consistent with the presence of partial melt in the shallow mantle. The regression fits indicate that the Pn intercept time is quite small (6.03 ± 1.11 s). This would imply a thin crust (~12 km) and a short Pn-Pg crossover distance (< 100 km). However, Pg appears to be the first arrival at station QURS (Figure 2), implying a thicker crust. A crustal thickness of about 30 km for the Dead Sea region is reported from studies of seismic refraction data (Ginzburg et al., 1979) and teleseismic receiver functions (Sandvol, et al., 1998). The inclusion of data from station QURS may be problematic if the structure to the east of the Dead Sea is dramatically different from that to the south.

We developed a velocity model for the paths considered by using a grid search scheme to fit the travel time data shown in Figure 3. A wide range of models was generated and the mean and root-mean square (rms) of the residuals (data minus the model prediction) were computed. The sensitivity of travel times to one-dimensional (1D) average velocity structure is certainly non-unique and our goal is to find a range of models that fit the data reasonably well and are consistent with what is already known about the region. By using a grid search technique we avoid problems associated with linearizing the dependence of the data on model parameters, as is required by linear inversion methods. Because the calculation of travel times in a 1D model is fast, the grid search allows us to quickly investigate a wide range of models. The best models were

chosen to minimize the absolute mean residual while also providing good scatter reduction.

We began by searching over a wide range of crustal velocity models and iterated to narrow the range. Figure 4 shows the models used in the grid search after narrowing the range of model parameters. We assumed a 2 km thick sediment layer for all models (Seber et al., 1997). The scaling between P- and S-waves assumed a Poisson's Ratio of 0.25, consistent with low velocity felsic compositions (Christensen and Mooney, 1995; Rudnick and Fountain, 1995). The total crustal thickness was varied from 22 to 36 km with a 2 km increment. Three layers composed the crystalline crust: an upper crust (5 km thickness, $v_p = 5.4\text{-}5.7\text{ km/s}$, 0.1 km/s increment); a middle crust (10 km thickness, $v_p = 5.8\text{-}6.2\text{ km/s}$, 0.1 km/s increment); and a lower crust (variable thickness, $v_p = 6.0\text{-}6.4\text{ km/s}$, 0.1 km/s increment). The mantle P-wave velocity was set to 7.8 km/s, consistent with the regression value (Figure 3).

We performed the grid search using travel time data sets: (a) Pn and Pg; and (b) Pn, Pg and Sg. We considered two data sets for two reasons. Firstly, the onset times of Sg are more difficult to pick, so it may not be prudent to include the Sg picks in the estimation of structure. Secondly, we are not directly solving for the shear wave velocities, but rather scaling shear velocities to compressional velocities with an assumed Poisson's Ratio, so the influence of Sg travel times may bias the model. The optimal model should reduce the scatter in the data (i.e. minimize the rms) and result in zero-mean residuals. We chose models that resulted in absolute mean residuals less than 0.5 seconds and minimum rms. The threshold on the absolute mean residual was chosen to be a conservative estimate on the picking error. From the 800 models considered we chose the 20 best fitting models according to the criteria described above. The 20 best-fitting models for both data sets are shown in Figure 4. Both data sets infer similar velocity models, however the models inferred from Pn and Pg data are less scattered. Crustal thicknesses range between 24 and 30 km. The upper crustal velocities are poorly resolved by both data sets. Velocities of the lower crust are 6.0-6.2 km/s.

The absolute mean residual is plotted versus the rms residual for both data sets in Figure 5. This figure illustrates how each model performs toward the goal minimizing the absolute mean residual and residual scatter. Figure 6 shows the fit of the 20 best-fitting models to the Pn, Pg and Sg travel times for the case when all three phases are fit simultaneously. One can see that the data are only weakly sensitive to changes in the crustal velocities. Comparison with the error bars shows that the theoretical travel time curves pass within two standard deviation of observed travel times. Thus, based on travel times alone, we cannot reject any of these models at the $2\text{-}\sigma$ level.

In order to select a single velocity model to be representative of the paths sampled, we appeal to the results of seismic refraction (Ginzburg et al., 1979) and a recent composite model of crustal thickness (Seber et al., 1997). Our grid search results with the thicker crusts (28-30 km) are consistent with these earlier studies. The preferred model has a crustal thickness of 28 km and is compiled in Table 3.

Conclusions

In this report we estimated a one-dimensional path-averaged crustal velocity structure for the Dead Sea Rift region. Travel times from two explosions in the Dead Sea provided clear observations of Pn, Pg and Sg phases at seismic stations in northwestern Saudi Arabia. The locations and origin times of the Dead Sea shots provided excellent ground truth for the analysis. However, because of trade-offs inherent to travel time modeling, we could not uniquely estimate the crustal structure and had to appeal to previous seismological studies to constrain the crustal thickness.

Our preferred model (Table 3) features a thin crust (crustal thickness 26-30 km) and low velocities (average P-wave velocity 5.8-6.0 km/s), consistent with the extensional tectonics of the region and previous studies (Ginzburg et al., 1979; Sandvol et al., 1998). Below the Moho, the P-wave velocity is 7.8 km/s, lower than the global average, but consistent with actively deforming continental regions. We did not observe regional Sn phases, however this could be due in part to the nature of the explosion

sources or attenuation of short-period mantle S-waves reported in previous studies (Kadinsky-Cade et al, 1986; Rodgers et al., 1997). Future work will focus on testing our model by performing travel time and location experiments using ground truth locations of mining explosions in the region. If additional data warrants, we will adjust the model. Finally, the model will be tested in network operations for routine locations.

Acknowledgements

AR is grateful to the staffs of KACST and KSU for their hospitality during a visit in November 1999. This work was performed in part under the auspices of the U.S. Department of Energy by the Lawrence Livermore National Laboratory under contract W-7405-ENG-48. This is LLNL contribution UCRL-ID-??????.

References

Al-Amri, M. S. and A. M. Al-Amri (1999). Configuration of the Seismographic networks in Saudi Arabia, *Seism. Res. Lett.*, 70, 322-331.

Christensen, N. and W. Mooney (1995). Seismic velocity structure and composition of the continental crust: A global view, *J. Geophys. Res.*, 100, 9761-9788.

Ginzburg, A., J. Makris, K. Fuchs, C. Prodehl, W. Kaminski and U. Amitai (1979). A seismic study of the crust and upper mantle of the Jordan-Dead Sea Rift and their transition toward the Mediterranean Sea, *J. Geophys. Res.*, 84, 1569-1582.

Hearn, T. and J. Ni (1994). Pn velocities beneath continental collision zones: the Turkish-Iranian Plateau, *Geophys. J. Int.*, 117, 273-283.

Kadinsky-Cade, K., M. Barazangi, J. Oliver and B. Issacks (1981). Lateral variations of high-frequency seismic wave propagation at regional distances across the Turkish and Iranian Plateaus, *J. Geophys. Res.*, 86, 9377-9396.

Kennett, B. and E. R. Engdahl (1991). Travel times for global earthquake location and phase identification, *Geophys. J. Int.*, 105, 429-465.

Myers, S. C., W. R. Walter, K. Mayeda and L. Glenn (1999), Observations in support of Rg scattering as a source of explosion S waves: regional and local recordings of the 1997 Kazakhstan depth of burial experiment, *Bull. Seism. Soc. Am.*, 89, 544-549.

Rodgers, A., J. Ni and T. Hearn (1997). Propagation characteristics of short-period Sn and Lg in the Middle East, *Bull. Seism. Soc. Am.*, 87, 396-413.

Rudnick, R. and D. Fountain (1995). Nature and composition of the continental crust: a lower crustal perspective, *Rev. Geophys.*, 33, 267-309.

Sandvol, E., D. Seber, A. Calvert and M. Barazangi (1998). Grid search modeling of receiver functions: Implications for crustal structure in the Middle East and North Africa, *J. Geophys. Res.*, 103, 26,899.

Seber, D., M. Vallve, E. Sandvol, D. Steer and M. Barazangi, 1997. Middle East tectonics: applications of geographical information systems (GIS), *GSA Today*, February 1997, 1-5.

Table 1. Ground Truth Locations from Geophysical Institute of Israel

LATITUDE	LONGITUDE	DATE	TIME (GMT)	YIELD (KG TNT)
31.5338	35.4400	Nov. 10, 1999	13:59:52.210	2060
31.5336	35.4413	Nov. 11, 1999	15:00:00.795	5000

Both shots were detonated in the water at 70-73 m depth.

These data were taken from the Geophysical Institute of Israel: <http://www.gii.co.il>.

Table 2. Automatic Locations of Dead Sea Shots by Saudi National Seismic Network

LATITUDE	LONGITUDE	DATE	TIME (GMT)	MISLOCATION (KM)
31.6214	35.1506	Nov. 10, 1999	13:59:58.807	29.1
31.8143	35.0178	Nov. 11, 1999	14:59:58.572	50.7

Table 3. Preferred Velocity Model for the Dead Sea Rift Region

DEPTH (KM)	THICKNESS(KM)	V_p (KM/S)	V_s (KM/S)
0.0	2	4.50	2.60
2	5	5.50	3.18
7	10	6.10	3.52
17	11	6.20	3.60
28	∞	7.80	4.37

V_p and V_s are the P- and S-wave velocities, respectively.

Figure Captions

Figure 1. Map of the ground truth shot location (star) and Saudi stations (triangles) that recorded the shots. The red circles indicate automatic locations of the shots by the KACST network.

Figure 2. Waveforms of the November 11, 1999 Dead Sea shot for (a) the KSU and (b) KACST Networks identified by station. Data were high-pass filtered with a corner frequency of 0.5 Hz.

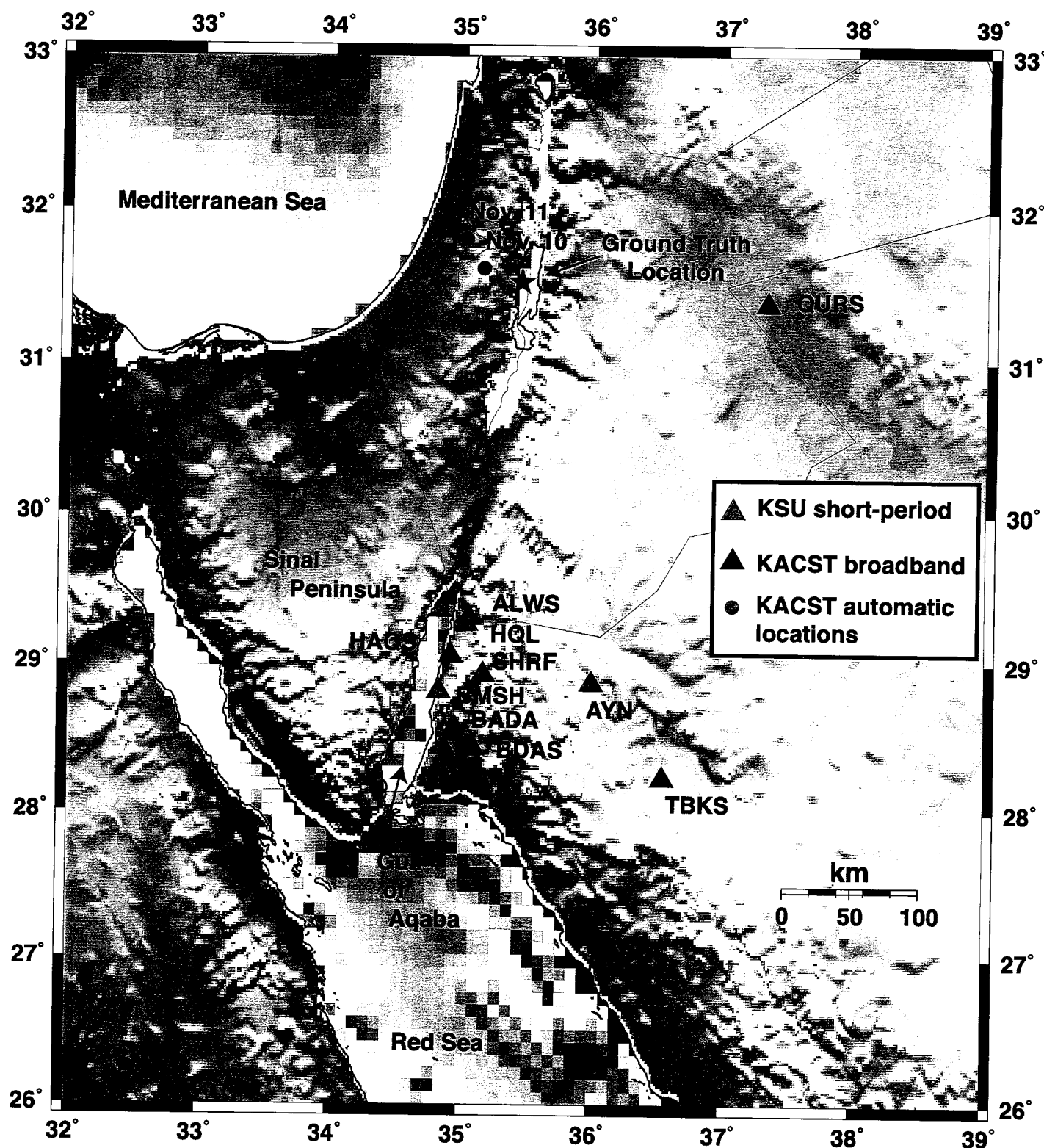
Figure 3. Travel times of Pn, Pg and Sg versus distance for the Dead Sea shots. The regression model and 1- σ errors are given in the figure and plotted.

Figure 4. P-wave velocity models investigated in the grid search (thin gray lines). The 20 best-fitting models are also shown (thicker black lines) for two travel time data sets (a) Pn and Pg; and (b) Pn, Pg and Sg.

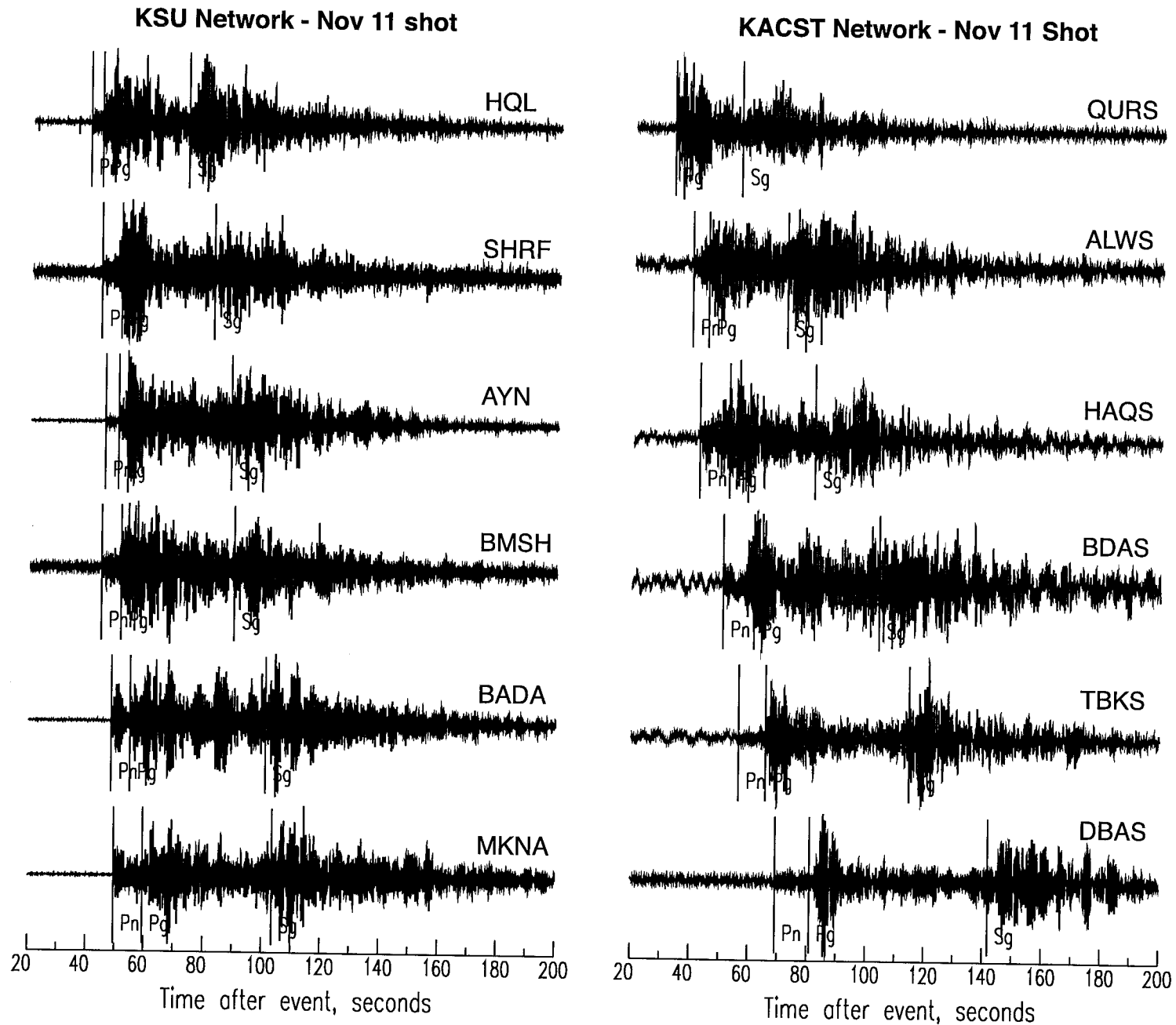
Figure 5. Plot of absolute mean and root-mean square (rms) residual for each model plotted in Figure 4 (open circles). The gray circles indicate the best-fitting models chosen to have an absolute mean less than 0.5 seconds and a minimum rms. Cases for two data sets are shown: (a) Pn and Pg; and (b) Pn, Pg and Sg.

Figure 6. Observed Pn, Pg and Sg travel times (symbols), 2- σ errors and the predictions of the best 20 models when all three phases are considered together (lines). The inset figure shows the best-fitting models.

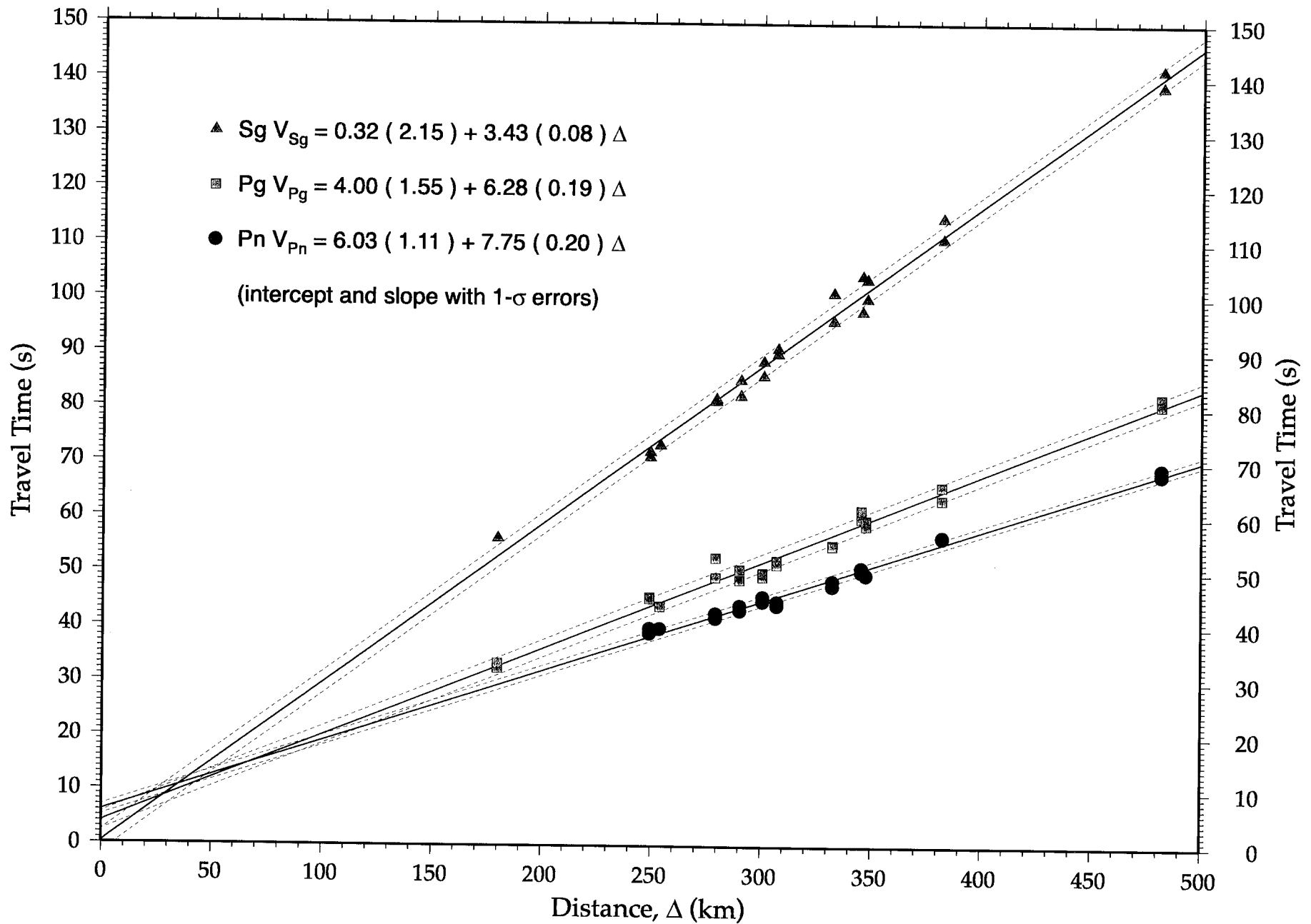
Saudi Seismic Networks and the November 1999 Dead Sea Shots



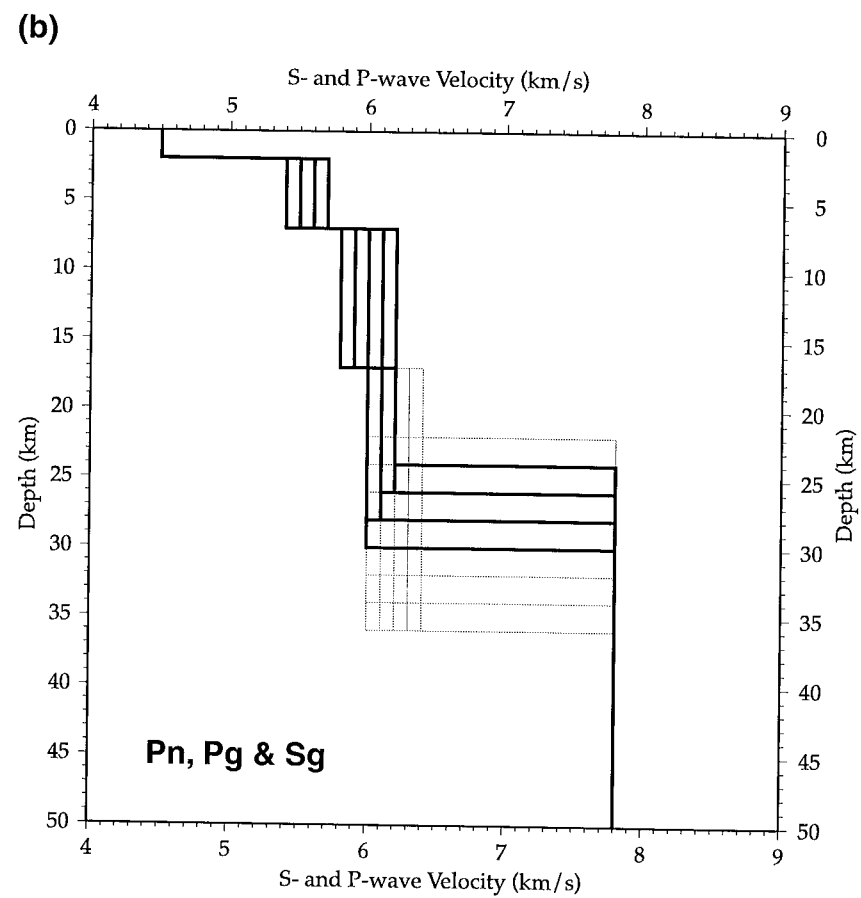
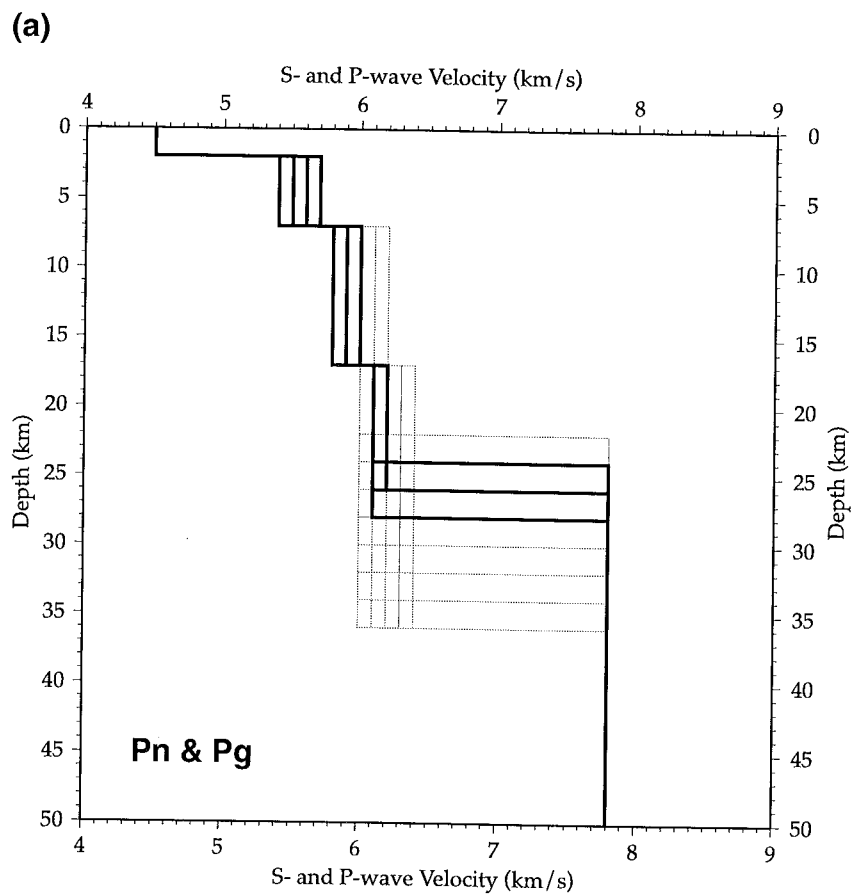
Rodgers et al., 2000, Saudi Observations of the Dead Sea Shots, Figure 1



Rodgers et al., 2000, Saudi Observations of the Dead Sea Shots, Figure 2

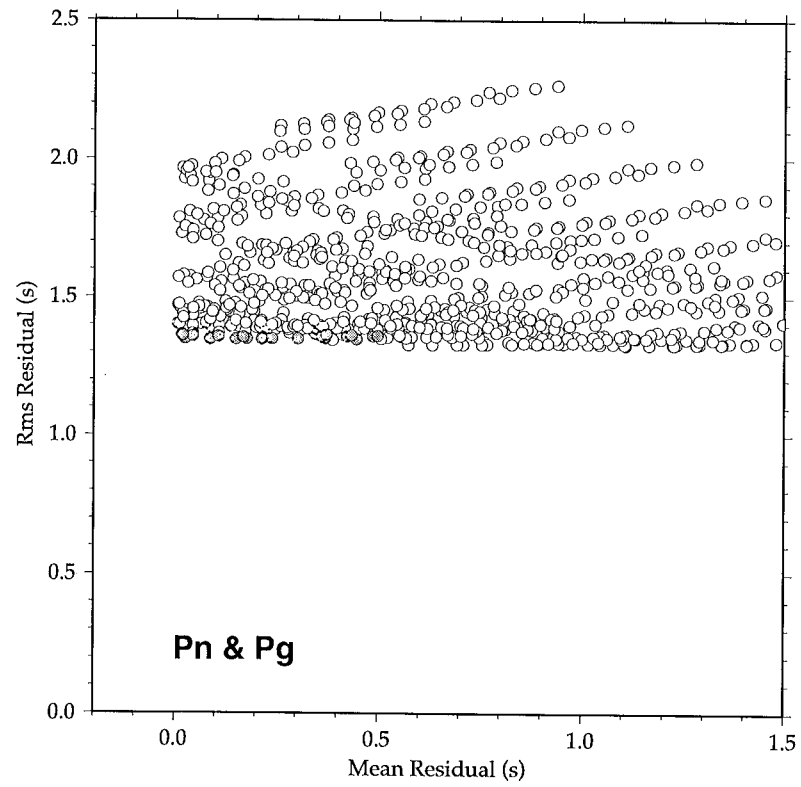


Rodgers et al., 2000, Saudi Observations of the Dead Sea Shots, Figure 3

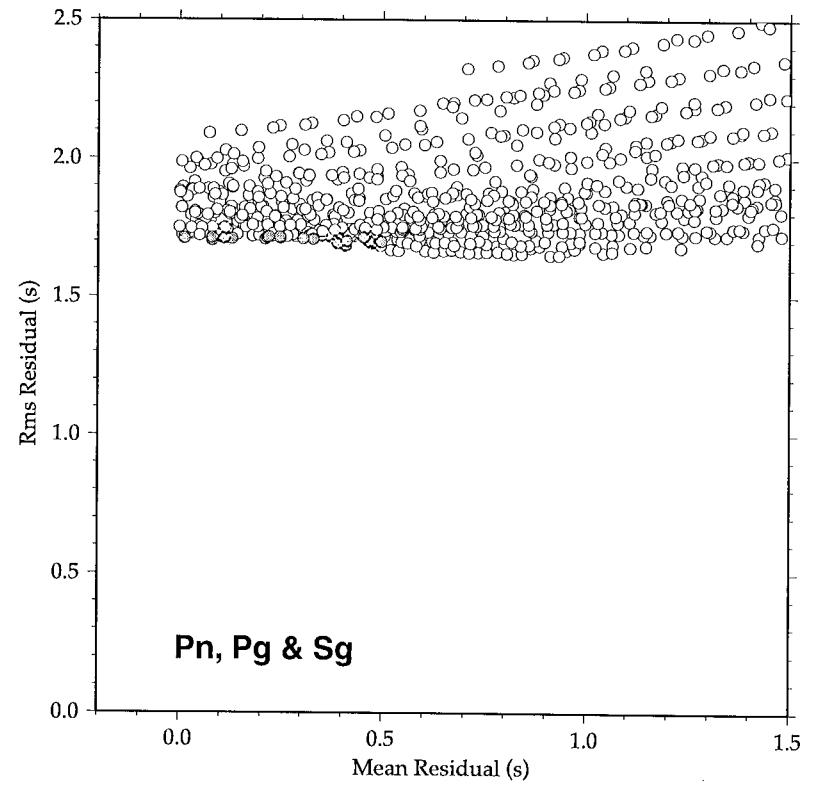


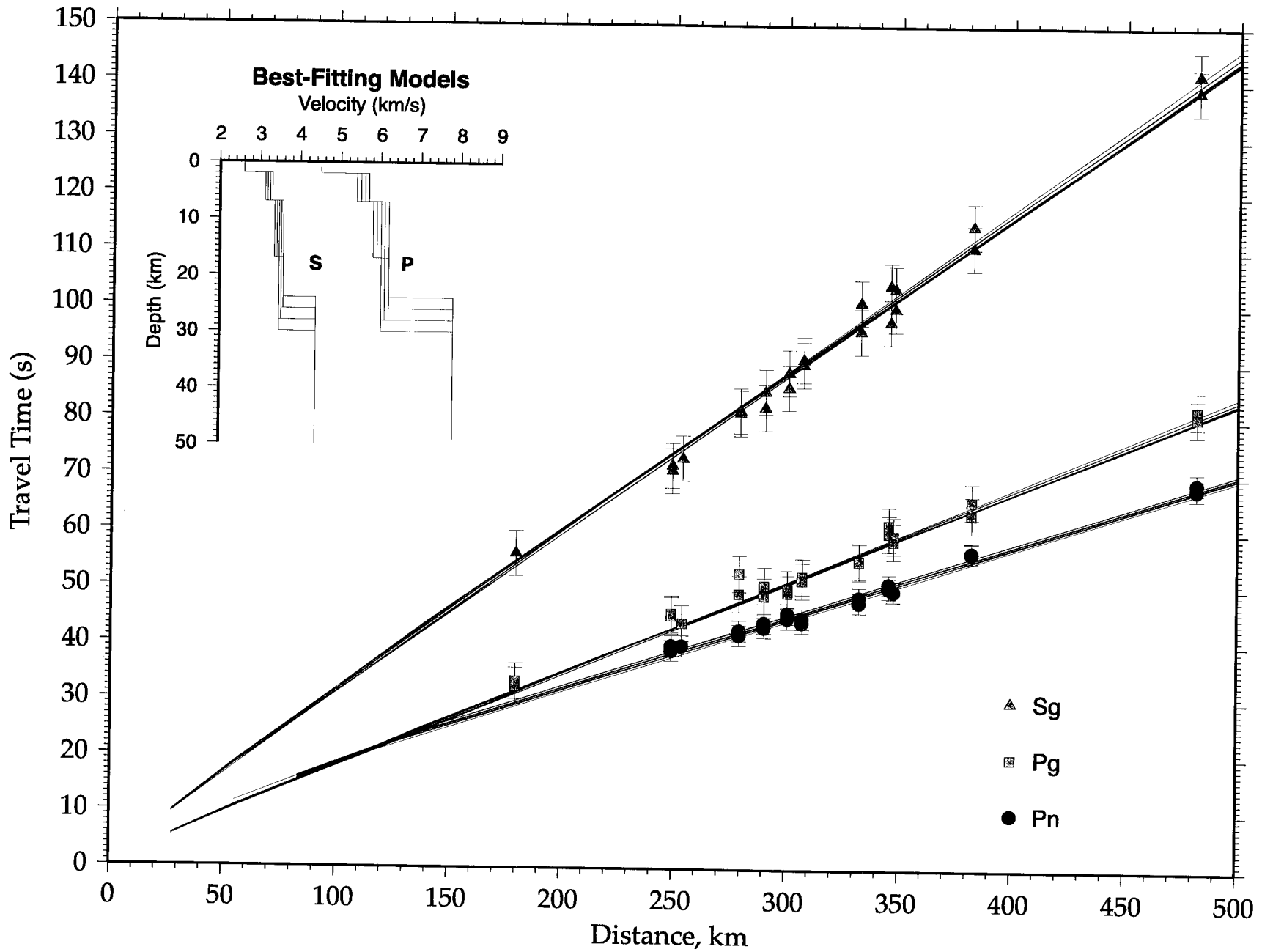
Rodgers et al., 2000, Saudi Observations of the Dead Sea Shots, Figure 4

(a)



(b)





Rodgers et al., 2000, Saudi Observations of the Dead Sea Shots, Figure 6